Available online at www.sciencedirect.com
SCIENCE DIRECT
Polymer 47 (2006) 6226–6235
polymer
www.elsevier.com/locate/polymer

Mechanical and swelling properties of PDMS interpenetrating polymer networks

Seong Hyun Yoo [a,1], Claude Cohen [a,*], Chung-Yuen Hui [b]

[a] School of Chemical and Biomolecular Engineering, 120 Olin Hall, Cornell University, Ithaca, NY 14853-5201, USA
[b] Department of Theoretical and Applied Mechanics, Cornell University, Ithaca, NY 14853, USA

Received 1 March 2006; received in revised form 7 June 2006; accepted 9 June 2006
Available online 7 July 2006

Abstract

Poly(dimethylsiloxane) (PDMS) interpenetrating networks (IPNs) of two different molecular weight PDMS were prepared. Six series of IPNs were obtained by first tetra-functionally end-linking long vinyl-terminated PDMS (molar mass 23×10^3 or 21×10^3 g mol^{-1}) neat or in a 50% solution with unreactive PDMS chains. These networks were then dried and swollen with short reactive telechelic PDMSs (molar mass 800, 2.3×10^3 or 5.7×10^3 g mol^{-1}) that were subsequently end-linked. The mechanical, toughness and swelling properties of these IPNs were investigated. We found that the correlation between modulus (E) and equilibrium swelling (Q) in toluene of the PDMS IPNs obeys a scaling relation identical to that of a normal unimodal PDMS network. This result strongly suggests effective load transfer between the networks. The results of the elastic modulus and of the toughness of the networks represented by the energy required to rupture them were analyzed in terms of a recent model by Okumura [Europhys Lett 2004;67:470.]. Although the modulus results are in reasonable agreement with the equal-stress model of Okumura, the toughness results are not. In addition, our measured toughness decreases instead of increases with composition in an opposite trend to that predicted by the equal-strain model. An empirical model based on fracture mechanics gives a good representation of the toughness data.
© 2006 Elsevier Ltd. All rights reserved.

Keywords: PDMS; IPN; Toughness

1. Introduction

Interpenetrating polymer networks (IPNs) consist of two polymeric components that are separately cross-linked into two interpenetrated networks with no chemical bonds between them. The great interest in IPNs stems from the potential of designing materials with a range of properties and perhaps generating a synergistic effect on one or more of the properties.

There are two ways of synthesizing IPNs: sequential cross-linking and simultaneous cross-linking. A sequential IPN is formed by polymerizing the first mixture of monomer, cross-linking agent, and initiator or catalyst to form a network; the network is then swollen with the second combination of monomer and cross-linking agent and polymerized to form an IPN. Reactive polymer chains instead of monomers can also be used along with initiator or catalyst to synthesize the networks. A simultaneous IPN is formed by polymerizing two different monomers or by using two different polymer chains along with complementary cross-linking agent pairs together in one step. The key to the success of this process is that the two components must polymerize or cross-link by reactions that will not interfere with one another. This is often accomplished by polymerizing one network by a condensation reaction, while the other network is formed by a free radical reaction.

IPNs have found widespread use in important materials such as sheet-molding compounds (SMCs), selective/permeable membranes, dental fillings, sound and vibration damping, tough rubber and plastic materials, ion-exchange resin, impact-modifier for thermoset materials, rimplast thermoplastics, pressure-sensitive adhesives, coatings materials and artificial joints [1].

* Corresponding author.
E-mail address: cc112@cornell.edu (C. Cohen).
[1] On leave from LS Cable, Seoul, South Korea.

0032-3861/$ - see front matter © 2006 Elsevier Ltd. All rights reserved.
doi:10.1016/j.polymer.2006.06.035

Poly(dimethylsiloxane) (PDMS) is the major building block of many silicone fluid-based products and silicone elastomers. The properties of PDMS can be modified by the substitution of the methyl groups on the silicon atom by hydrogen, alkyl, phenyl, or organo-functional groups. Due to their unique properties polysiloxanes have applications in medical, electric, electronic, automotive and other industries [2]. The properties of PDMS networks obtained by end-linking di-functional vinyl-terminated precursor chains to tetra-functional silanes have been well studied, but the properties of PDMS–PDMS interpenetrated networks have not received much attention since the work of Mark and Ning 20 years ago [3]. These authors studied both simultaneous PDMS IPN and sequential IPN. They found that sequential IPNs formed from two different molar masses have limited extensibility, whereas simultaneous IPNs have unusually large extensibilities, making their energies for rupture comparable to those of the corresponding interconnected bimodal networks. None of the previous researchers on interpenetrated PDMS networks investigated the modulus–swelling correlation and toughness enhancement factors of these networks in a quantitative way.

Our interest in IPNs was stimulated by a recent theoretical paper by Okumura [4] on the modulus and toughness of such networks. Okumura makes predictions on both the elastic modulus and the toughness of these interpenatrating networks based on the elastic properties of each of the individual network and on the composition of the interpenetrating network. Predictions for the modulus and the toughness of the IPN under uniaxial deformation are made assuming that the two independent networks of the IPN are either under an equal-stress condition or under an equal-strain condition. The synthesis of end-linked PDMS IPNs has allowed us to test some of these predictions. In addition, we have also examined the swelling properties of PDMS IPNs in toluene.

2. Experimental procedures

2.1. Synthesis of precursor chains

With the exception of the 800 g mol^{-1} vinyl-terminated PDMS precursor chains that were purchased from Gelest, Inc., all other vinyl-terminated precursor chains (2300, 5700, 21,000 and 23,000 g mol^{-1}) were synthesized from hexamethylcyclotrisiloxane monomer (Gelest, Inc.) by anionic ring opening polymerization in a 50 wt% toluene solution at 60 °C using benzyltrimethylammoniumbis(*o*-pheny1enedioxy)-phenylsiliconate as a catalyst and dimethylsulfoxide (DMSO) as a promoter. Calculated amounts of HPLC water based on an empirical calibration curve were added to control the molar mass of the resulting polymer. After the polymerization, pyridine, an acid scavenger was added to the resulting polymer/toluene mixture. The living chains were end-capped with vinyl groups by adding vinyldimethylchlorosilane. The polymer samples thus obtained were washed with water, dissolved, and reprecipitated with toluene and methanol, and then dried in a vacuum oven at 60 °C for 3 days. The details of the catalyst preparation and the synthesis of polymer are reported elsewhere [5–8].

The PDMS polymers were characterized by gel permeation chromatography (GPC) to determine the molar mass and its distribution. The GPC was calibrated using polystyrene standards and toluene was used as the carrier solvent. The molar mass obtained was corrected to PDMS equivalent by using a calibration developed by Lapp et al. [9]. Four different molar mass PDMSs were synthesized in this study. Their number average molar masses were 23,000, 21,000, 5700 and 2300 g mol^{-1}, and their polydispersity indexes were determined to be 1.33, 1.36, 1.19 and 1.13, respectively. The large molar mass precursors were used for the base networks to be swollen by the short chains for the formation of the IPNs.

2.2. Synthesis of base networks

Base networks were formed by end-linking the long-chain PDMS (M_n of 23k and 21k) with the tetra-functional cross-linker tetrakis(dimethylsiloxy)silane in the presence of a platinum catalyst [10–12]. The optimum amount of cross-linker tetrakis(dimethylsiloxy)silane was added to the polymer mixture and the reaction was catalyzed by *cis*-dichlorobis(diethyl sulfide)platinum(II) in toluene. Based on a previous study [13,14], the optimal molar ratio r of silane hydrogens to vinyl groups was fixed at 1.7 for the networks considered here. The 21k PDMS base networks were formed in solution with non-reactive trimethoxy-terminated PDMS solvent to reduce the modulus of the base network and to provide a larger difference in moduli between the two interpenetrated networks. The networks were allowed to cure at 35 °C for 3 days in Teflon® molds. The trimethoxy-terminated PDMS solvent and the soluble fraction were then extracted from the networks by swelling in toluene. The weight fraction of the soluble material and the equilibrium swelling ratio in toluene of the base networks were determined using standard gravimetric procedures [15]. Samples of uniform dimensions for the mechanical measurements were obtained by using a sample puncher.

2.3. Synthesis of PDMS IPNs

Samples of the extracted and dried base networks were swollen to various extents with short chains (molar mass 800, 2.3k, or 5.7k) and proper amount of the catalyst *cis*-dichlorobis(diethyl sulfide)platinum(II)/toluene solution. The networks were put in an oven at 30 °C to facilitate the swelling, and to evaporate the toluene present with the catalyst. For high concentration of absorbed short chains, more time was needed to swell the base networks with the short chain PDMS. After the networks were fully and uniformly swollen, a stoichiometric amount of cross-linker was incorporated with a small amount of toluene onto the inverse side of the network. The samples were put in a refrigerator overnight to allow the cross-linker to diffuse before extensive reaction takes place. After sufficient time had elapsed for homogeneity to be attained, the PDMS short chains were tetra-functionally

cross-linked by heating the samples to 35 °C for 2 days. Re-extractions and swelling gave soluble fractions from the second end-linking process and the equilibrium swelling ratios of the interpenetrated networks in toluene. The soluble fraction W_S of the IPN reported in Table 1 is based on the soluble amount extracted after the second end-linking step and is relative to the total mass of the IPN. Table 1 also lists the values of the equilibrium swelling ratio Q.

2.4. Mechanical and ultimate properties' measurement in extension

A Perkin–Elmer 7e Dynamic Mechanical Analyzer (DMA) was used to measure the Young's modulus of our samples. The networks after cure or the interpenetrating networks after reaction were punched using a sample puncher, and samples with uniform width and flat surfaces were obtained. Exact dimensions (4–5 mm in width, 0.5–1 mm in thickness and 7–10 mm in length) of the samples were measured using a micrometer. These data were entered into the DMA software to calculate the stress applied to the sample.

The Young's modulus of the samples is measured in the extension mode at a strain of about 1%. The region around 1% strain is in the linear region of the stress–strain diagram for rubber-like materials, and produces an accurately measurable strain. Ten different values of stresses were applied to give strains ranging from 0.7 to 1.5%. The Young's modulus of the sample was taken as the slope of the best-fit line to the data of stress versus strain. The modulus of at least three samples from the same IPN network was measured and the limits of the error bars in Fig. 3 indicate the maximum and minimum values obtained.

Table 1
IPNs composition and properties

M_n of base network	Vol% of trimethoxy-terminated PDMS solvent in base network	M_n of short chain	mol%, mass% of short chains	E (MPa)	Q	W_S (%)	Toughness[a] (MPa)	Maximum stress (MPa)
23k	0	800	0	0.63	4.13	1.6	0.49	0.45
			70, 6.1	0.66	4.03	1.9	0.54	0.48
			80, 13	0.68	3.90	0.0	0.52	0.51
			90, 23	0.87	3.46	1.9	0.13	0.34
			92.5, 30	0.94	3.35	1.7	0.14	0.37
			95, 40	1.04	3.23	1.9	0.068	0.35
			100	3.69	2.07	4.5	0.11	0.76
		2.3k	0	0.46	4.89	2.4	0.41	0.41
			70, 19	0.61	4.23	5.6	0.38	0.48
			80, 28	0.71	3.94	3.3	0.18	0.45
			90, 47	0.94	3.42	0.8	0.37	0.47
			92.5, 55	1.03	3.3	1.4	0.18	0.45
			100	2.19	2.42	0.33	0.15	0.59
		5.7k	0	0.63	4.13	1.6	0.73	0.50
			50, 21	0.80	3.85	3.7	0.39	0.48
			60, 29	0.84	3.73	1.8	0.29	0.45
			67, 33	0.88	3.57	1.1	0.33	0.45
			73, 38	0.95	3.49	1.9	0.20	0.42
			100	1.88	3.03	0.42	0.34	0.77
21k	50	800	0	0.22	7.96	0.6	0.28	0.17
			92.5, 32	0.52	4.11	2.8	0.37	0.47
			95, 45	0.71	3.42	1.1	0.23	0.39
			97.5, 62	0.96	3.37	1.3	0.083	0.30
			98.5, 74	1.11	2.91	1.4	0.058	0.30
			99, 81	1.36	2.73	1.3	0.060	0.34
			100	3.69	2.07	4.5	0.11	0.76
		2.3k	0	0.22	7.96	0.6	0.28	0.17
			80, 26	0.47	4.94	7.0	0.41	0.40
			85, 37	0.53	4.25	3.1	0.20	0.40
			90, 49	0.66	3.63	2.1	0.061	0.39
			95, 67	0.71	3.76	2.4	0.17	0.35
			100	2.19	2.42	0.33	0.15	0.59
		5.7k	0	0.22	7.96	0.6	0.28	0.17
			60, 29	0.25	6.69	2.1	0.39	0.24
			65, 30	0.40	4.91	7.1	0.41	0.25
			70, 36	0.50	4.66	6.4	0.30	0.36
			75, 44	0.65	4.30	1.7	0.19	0.33
			80, 52	0.71	4.47	0.6	0.27	0.42
			100	1.88	3.03	0.42	0.34	0.77

[a] Toughness reported is the maximum value observed in 4–7 samples (see text).

Engineering stress (force (f)/initial cross-section area (A^*)) versus extension ratio (final length/initial length) measurements were also taken using an automated Instron® uniaxial testing machine at room temperature. The dimensions of the specimens were 0.5–1 mm in thickness, 6–7 mm in width and 50–70 mm in length. Each sample was clamped in its undeformed state and then stretched at a strain rate of 20 mm/min until rupture. The values of the elastic modulus reported by the data acquisition system of the Instron were typically within a few percent of the values obtained with the DMA with the exception of the more brittle samples obtained solely from the short chains (800, 2.3k and 5.7k) where the discrepancy was of the order of 10%.

3. Results and discussion

3.1. Mechanical and swelling properties

The equilibrium Young moduli E and swelling ratios Q in toluene, defined as the ratio of the volume of a swollen network to its dry volume, of IPNs are summarized in Table 1. The modulus values E increase and the equilibrium swelling ratio Q decreases as expected with increasing mol% of short chains in the IPNs.

The results of the modulus (E) of the dry network and the degree of equilibrium swelling ratio (Q) in toluene of the various IPNs are listed in Table 1. Fig. 1 shows the data of E versus Q in a log–log plot. The best-fit line to the experimental data yields:

$$E \sim Q^{-1.88}$$

This power-law behavior is practically identical to previous reported results for unimodal PDMS networks with an exponent of −1.91 [14]. This may at first appear as a surprising result because the structure of the IPNs might be thought to be very different from that of unimodal networks. It is easily argued, however, that the unimodal networks end-linked in the melt state are highly self-interpenetrated as the volume of a polymer chain of molar mass 20,000 g mol^{-1} will contain approximately 5 other chains in the melt [15]. Once end-linked, these chains will be highly interpenetrated. The swelling results from the IPNs show that the two networks forming the IPNs cannot be treated as mechanically independent. As a consequence, there must be effective load transfer between the two networks.

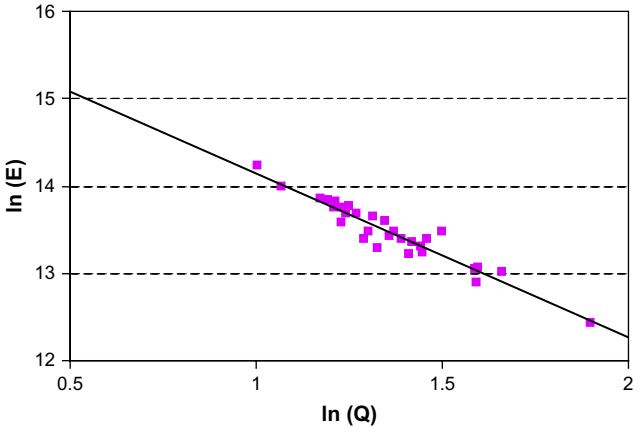

Fig. 1. Behavior of E versus Q for PDMS interpenetrating networks swollen in toluene. The slope of the best-fit line is −1.88.

The stress–strain curves for two of the PDMS IPNs series are presented in Fig. 2. The area under each curve is the energy density of rupture (E_r) that represents the standard measurement of toughness of an elastomer. Values of toughness in MPa are listed in Table 1 for the six series considered here. Four to seven samples were run for each specimen and the curves shown are the ones with the highest elongation. The stress–strain data of all the samples from a given specimen followed closely the same curve but broke at different elongations due to the inherent defects or improper mounting on the Instron. For consistency, the data presented are therefore for the maximum toughness observed among 4–7 samples of a given specimen. We expect that taking an average value of the toughness for a large number of identically prepared samples when the failure occurs at the mid-section of the sample (as opposed to near the grips or at other points of stress concentration) would lead to conclusions that would not significantly differ from those obtained here. A standard way to carry out toughness tests is to perform such tests on samples with a large

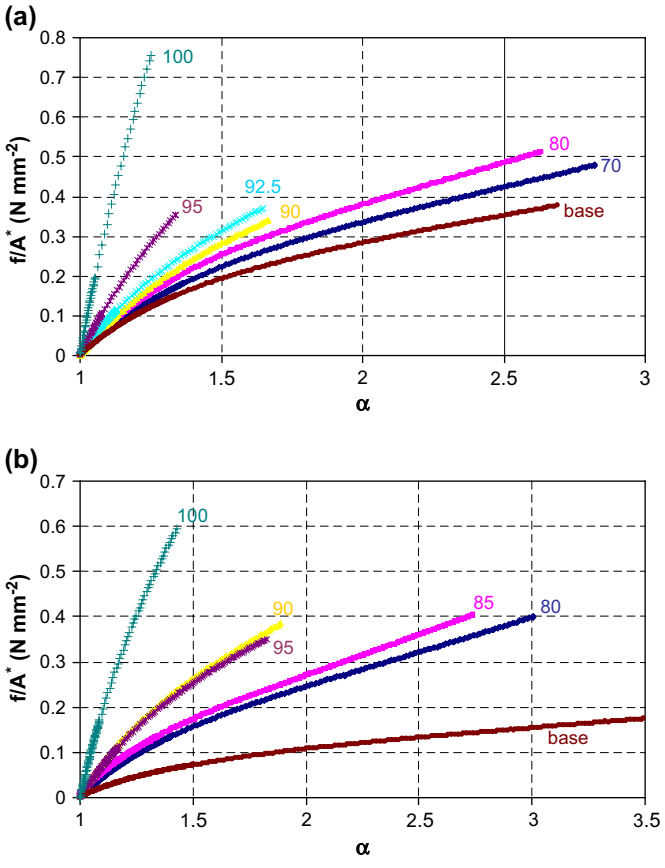

Fig. 2. Engineering stress (f/A^*) versus extension ratio curves of IPNs: (a) 800/23k IPNs; (b) 2.3k/21k (50% sol) IPNs. The value associated with each curve indicates the mol% of short chains in the IPN.

preexisting crack or tear introduced in the sample. We are currently investigating such procedures.

Toughness enhancement over the toughness of the long-chain base network in the IPNs was observed at moderate mol% short chain (70–85 mol%). The toughness values began to decrease as the proportion of short chains in IPNs increased (see Table 1). We note that in all the series, the experimentally determined maximum stress at break was always lower than that of the pure short chain networks.

3.2. Okumura's model and comparison with experimental results

Okumura's assumes that IPNs consist of two ''energetically independent'' networks, usually one is relatively much stiffer than the other. In a recent attempt to elucidate the properties of such materials based on their composition, Okumura [4] proposed a model to explain the toughness enhancement obtained by interpenetrating a soft network with a stiff network based on the properties of each of the two networks that make up the IPN (modulus or mesh size, maximum stress) as well as the composition of the IPN (volume fraction of its constituents). He presented results based on the assumption that the two networks of the IPN are subjected to either equal-stress or equal-strain. Under the equal-strain condition, the stress loaded on the IPN is determined by the contribution of the stress of each network according to their volume fraction. In this case (networks in parallel), the modulus of IPN will have linear relationship of the moduli of two networks weighted by their volume fraction (solid line in Fig. 3). Under the equal-stress condition (networks in series), the total strain that is proportional to the reciprocal modulus will be the average of the strain of each network based on their volume fraction. This leads to a dependence of the IPN modulus on volume fraction given by Eq. (2) below and represented by the dashed line in Fig. 3. It should be noted that the moduli obtained using the equal-stress and strain assumptions are the well-known Voigt and Reuss bounds, respectively [16]. Furthermore, it can be shown rigorously that the Voigt bound is a lower bound while the Reuss bound is an upper bound [17]. This is confirmed by our data that lie between these two bounds in Fig. 3.

We note that for the IPNs synthesized with short chains of 800 g mol^{-1}, with the exception of very high volume fractions ($\phi_S > 0.6$), the concentration of short chains is not sufficient to produce interpenatrating networks where the short chain network spans the entire volume. For the short chains of molar mass 2.3k and 5.7k, the overlap concentration under the theta conditions can be estimated roughly [18] to be 0.4 and 0.25, respectively. The experimental data ranges from low volume fractions of short chains (forming cross-linked clusters in the IPN) to high volume fractions (forming interpenetrating networks spanning the entire volume). Nonetheless, the modulus data are fairly continuous as a function of ϕ_S. Even though the smaller chains are not able to form a percolating network at low volume fractions, the formation of interpenetrated domains is sufficient to increase the modulus of the base network in a continuous way as a function of concentration.

The equal-stress model appears intuitively more appealing and consistent with the fact that short length scale deforms less affinely than longer length scale in a network [19] and therefore the short chains are expected to be less strained than the longer chains. Our experimental data on modulus–volume fraction relationship of the six series of IPNs investigated are shown in Fig. 3. The experimental modulus data are in general much closer to the prediction of the equal-stress condition. We summarize below Okumura's results of the constant stress model that we then use to quantitatively analyze our toughness data.

Each network component comprising an IPN is symbolically illustrated in Fig. 4. Under the equal-stress condition, the stress σ on the IPN is equal to the stress on both the long-chain network σ_L as well as the stress σ_S on the short chain network:

$$\sigma = \sigma_L = \sigma_S = E_L e_L = E_S e_S \tag{1}$$

where e_L and e_S represent the strain of each of the components, respectively. The modulus E of the IPN is then given by [4]:

$$\frac{1}{E} = \frac{\phi_L}{E_L} + \frac{\phi_S}{E_S} \tag{2}$$

The stress distribution of the IPN near the tip of a crack of length a in a macroscopic sample at incipient fracture is given by [20]:

$$\sigma(r) = \sqrt{\gamma E / r} \tag{3}$$

where r is the distance from the tip and γ is the fracture energy of the IPN. This equation based on continuum theory is valid only when the crack length and the distance r in Eq. (3) are larger than the largest mesh size, ξ_L. The maximum stress of the IPN is therefore cut off at ξ_L and is:

$$\sigma_m \sim \sqrt{\gamma E / \xi_L} \tag{4}$$

according to Eq. (3).

On the other hand, the failure stress of the short chain network in IPN is expressed as:

$$\sigma_S \sim \sqrt{\gamma_S E_S / a_S}, \tag{5}$$

where γ_S is the fracture energy of the short chain network and a_S is a size of a microscopic Griffith cavity in the short chain network with $\xi_S < a_S < \xi_L$. Assuming that the short chain network breaks before the long one and using the equal-stress assumption, Okumura sets the maximum failure stress of the IPN, σ_m, to equal the inherent failure stress σ_S:

$$\sigma_m \sim \sigma_S. \tag{6}$$

Comparison of Eqs. (4) and (5) then yields:

$$\gamma \sim \frac{\xi_L}{a_S} \frac{E_S}{E} \gamma_S. \tag{7}$$

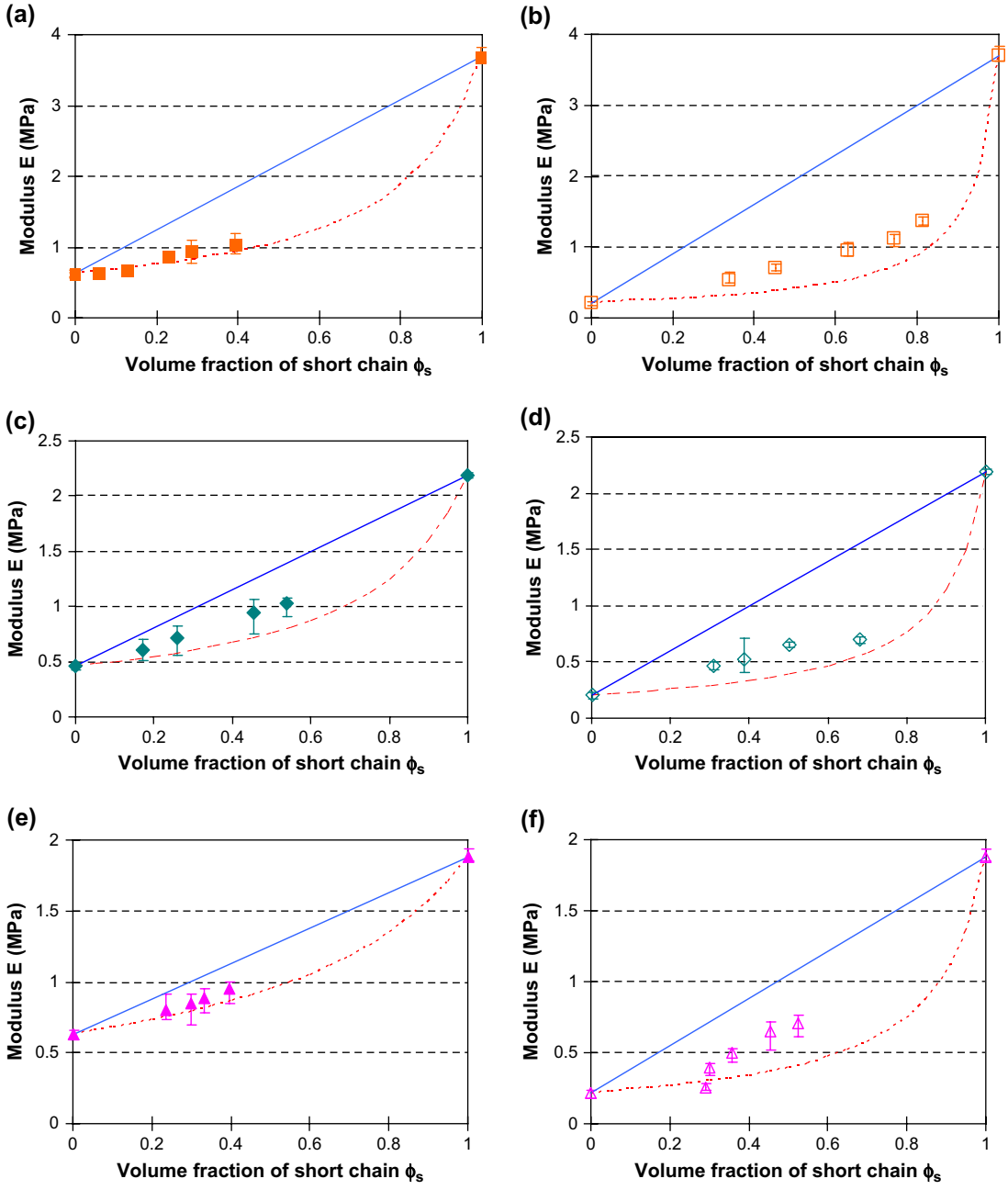

Fig. 3. Elastic modulus versus volume fraction of short chain in IPNs: (a) 800/23k, (b) 800/21k (50% solvent), (c) 2.3k/23k, (d) 2.3k/21k (50% sol), (e) 5.7k/23k, (f) 5.7k/21k (50% solvent), solid line: $E = \phi_S E_S + \phi_L E_L$ (equal-strain condition, Ruess bound), and dashed line: $1/E = \phi_S/E_S + \phi_L/E_L$ (equal-stress condition, Voigt bound).

The enhancement factor of the toughness of the IPN over that of the short chain network is obtained by combining Eqs. (2) and (7):

$$\lambda \equiv \frac{\gamma}{\gamma_S} = \frac{\xi_L}{a_S}\left(\phi_S + \phi_L \frac{E_S}{E_L}\right). \tag{8}$$

According to Eq. (8), the most critical factor in the toughness enhancement besides the composition and ξ_L is the modulus ratio of the two networks forming the IPN. Note that for large E_S/E_L, Eq. (8) implies that toughness enhancement is proportional to $\phi_L = 1 - \phi_S$, which suggested that toughness enhancement decreases with increase in mol% of short chains, not entirely consistent with our experimental observations (see Table 1). On the other hand, the prediction from the constant strain model is even less favorable. This model [4] predicts that λ would increase with $(\phi_S E_S + \phi_L E_L)/E_S$. Our data presented in Fig. 5 show that, in general, an opposite trend is observed.

The theoretical work of Okumura was motivated largely by the intriguing experimental results of Gong et al. on super-tough hydrogels [21,22]. To our knowledge, the structure of these gels is not well-defined and the determination of the necessary parameters from these gels to test the model is elusive.

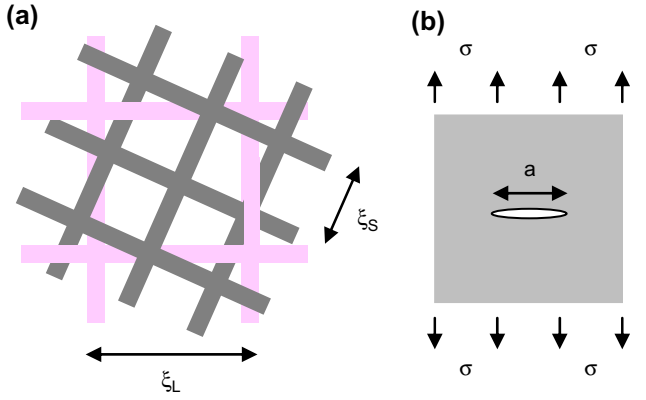

Fig. 4. Illustration representing an IPN made up of a short chain network "S" and a long-chain network "L" with mesh sizes ξ_S and ξ_L, respectively, (b) illustration of a crack of size a in a continuum subjected to a tensile stress σ.

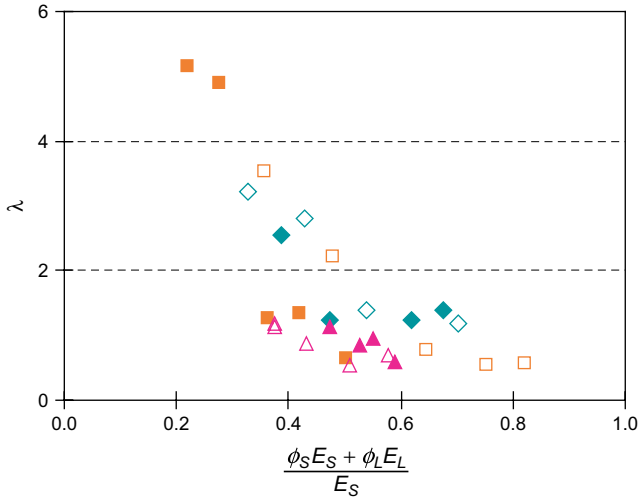

Fig. 5. Plot of the enhancement factor based on the equal-strain model. The data symbols are for the following IPNs (■) 800/23k; (◆) 2.3k/23k; (▲) 5.7k/23k; (□) 800/21k; (◇) 2.3k/21k; (△) 5.7k/21k. The 21k base networks were prepared in 50% solvent.

Our interpenetrating PDMS networks on the other hand are synthesized from well-established end-linked chemistry that is known to lead to well-defined structures and the properties of the base networks have been studied extensively.

Fig. 6 shows the plot of our experimental data based on Eq. (8). High toughness enhancement was found when the molar mass difference of the two precursor chains making up the two networks of the IPN is large (high E_S/E_L), in qualitative agreement with Eq. (8). Furthermore, the experimental data in Fig. 6 appear to be clustered in two groups according to the long-chain base network. All the data for the 23k base network fall reasonably well on a straight line. The data for the 21k base networks are more spread out. Nonetheless, the effect of the parameter a_S in Eq. (8) appears negligible and independent of the molar mass of short chains (at least in the range of molar mass studied here). This implies that the only relevant microstructural factor in Eq. (8) is the mesh size ξ_L of the long chains. The 21k long-chain network end-linked in a 50% solvent should have a larger ξ_L than that of 23k network

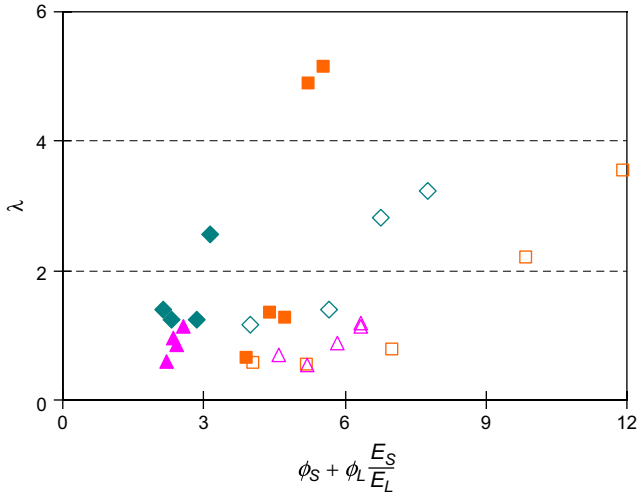

Fig. 6. Plot of the enhancement factor based on the equal-stress model, Eq. (8). The data symbols are for the following IPNs (■) 800/23k; (◆) 2.3k/23k; (▲) 5.7k/23k; (□) 800/21k; (◇) 2.3k/21k; (△) 5.7k/21k. The 21k base networks were prepared in 50% solvent.

and has lower modulus value. According to Eq. (8) the data from IPNs formed with 21k (in 50% solvent) base network as plotted in Fig. 6 must have a higher slope than those of the 23k base network IPNs. Our results, however, show the opposite trend.

Okumura [4] assumed that the short chain network breaks before the long one and took the maximum stress of the IPNs as that of the short chain network. It should be noted that this assumption is somewhat inconsistent with his equal-stress assumption, i.e., Eq. (6). Indeed, if the stresses acting on the soft and hard chains are equal, then it is difficult to understand why short chains will break before the long ones. Our results indicate, however, that the rupture of all the IPN series is governed by the maximum stress of the long-chain base network because IPNs with 23k base network showed higher stress at break than those with 21k (prepared in 50% solvent) at the same molar mass and similar mol% of short chains.

Of course, the fact that the equal-stress assumption leads to a satisfactory estimate of the composite modulus E does not imply that such an assumption can be used to study fracture, which is primarily governed by local processes. Indeed, it is well-known that the fracture behavior of a material can be affected dramatically by very small changes in local microstructure with negligible effect on the elastic modulus. Therefore, the equal-stress assumption, expressed by Eq. (6), is likely to be incorrect near the crack tip. In addition, our swelling experiment strongly suggested that there is effective load transfer between the stiff and soft networks, contrary to the hypothesis of Okumura, who assumes that the two networks are energetically independent. Therefore, it is not surprising that the toughness enhancement factor given by Eq. (8) fails to capture the failure characteristic of our samples.

A simple way to resolve this situation is to abandon the assumption of equal-stress assumption and to note that if the failure of our specimens is caused by the growth a major

defect of length a, then at failure, we must have, using a standard result in fracture mechanics,

$$\sqrt{\gamma E} \approx \sigma_{\max}\sqrt{a}, \tag{9}$$

where $\sigma_{\max}$ is the maximum stress in the tension test. It should be noted that the size of the defect a can be a function of the composition. Eq. (9) is also valid for the case where $\phi_S = 1$, i.e.,

$$\sqrt{\gamma_S E_S} \approx \sigma_{\max,s}\sqrt{a(s)}, \tag{10}$$

where $a(s)$ is the size of a macroscopic flaw and $\sigma_{\max,s}$ is the maximum stress in a tensile test of a sample consisting entirely of stiff chains. As commented above, $a(s)$ needed not to be the same as a. Dividing Eq. (9) by Eq. (10) results in

$$\gamma/\gamma_S \cong \frac{a}{a(s)}\left(\phi_S + \phi_L\frac{E_S}{E_L}\right)\left(\frac{\sigma_{\max}}{\sigma_{\max,s}}\right)^2, \tag{11}$$

where we have used Eq. (2) to compute E_S/E. Despite the scatter in the data, the results shown in Fig. 6 indicate an insensitivity to the parameter $a(s)$ for a given base long-chain network and a dependence on the properties of the long-chain network (ξ_L, $\sigma_{\max,L}$). We therefore assume the empirical relation:

$$\frac{a}{a(s)}\sigma_{\max}^2 = b\xi_L\sigma_{\max,L}^2, \tag{12}$$

where b is a proportionality factor with unit of inverse length that is independent of the mesh sizes of both networks and $\sigma_{\max,L}$ is the maximum stress in a tensile test of a sample consisting entirely of long chains. The toughness enhancement factor based on Eq. (12) is then written as:

$$\gamma/\gamma_S \cong b\xi_L\left(\phi_S + \phi_L\frac{E_S}{E_L}\right)\left(\frac{\sigma_{\max,L}}{\sigma_{\max,s}}\right)^2, \tag{13}$$

As shown in Fig. 7, Eq. (13) gives a reasonably good description of the effect of ξ_L on the toughness enhancement. This result is consistent with our earlier comment that the rupture of our IPN samples is governed by the maximum stress of the long-chain base network. In Gaussian networks, the mesh size ξ is related to the molar mass between effective cross-link M_c by:

$$M_c \sim \xi^2 \tag{14}$$

and the relationship between modulus and M_c is:

$$E = \frac{3\rho RT}{M_c}. \tag{15}$$

Therefore, ξ will be proportional to $(1/E)^{1/2}$. The predicted slope ratio of the 21k (end-linked in 50% solvent) base network IPNs to the 23k base network IPNs will be 1.7 because the moduli of the base networks are 0.22 and 0.63 MPa, respectively. Our experimental value of the ratio of slopes in Fig. 6 is 1.9, which is not too far from 1.7 given the uncertainties of the best-fit slopes in Fig. 7.

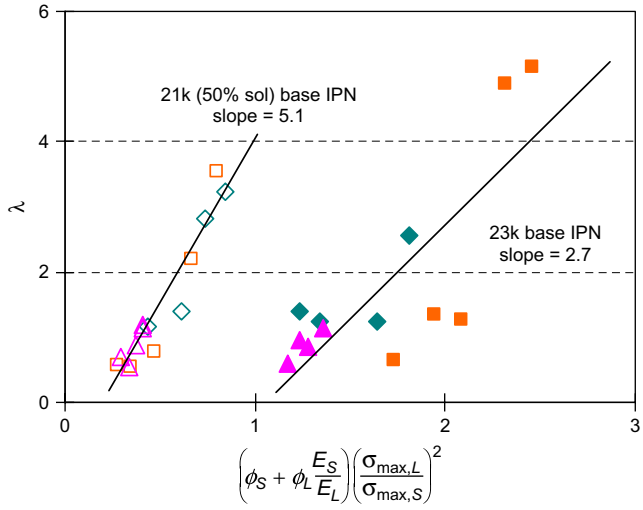

Fig. 7. Plot of the enhancement factor based on the modified equal-stress model, Eq. (13). The data symbols are for the following IPNs: (■) 800/23k; (◆) 2.3k/23k; (▲) 5.7k/23k; (□) 800/21k; (◇) 2.3k/21k; (△) 5.7k/21k. The 21k base networks were prepared in 50% solvent.

In Table 2, the values of the Mooney–Rivlin coefficients $2C_1$ and $2C_2$ are listed for all the samples examined. To extract these values, experimental data of the type shown in Fig. 2 are plotted according to

$$f^* = \frac{f}{A^*(\alpha - \alpha^{-2})} = 2C_1 + 2C_2/\alpha$$

and the coefficients are extracted from the portion of the data that give a linear plot of f^* versus α^{-1}. We note that the value of C_1 that represents the covalent cross-links' contribution to the modulus [18] increases fairly systematically as the amount of short chains increases in any given IPN series as would be expected because of the increase in the average number density of cross-links in the samples. The value of C_2, on the other hand, appears almost unchanged as a function of short chain concentration in the 23k base network but increases for the 21k base networks. Because C_2 has been related to the effect of entanglements (and interdispersion), we may conclude that short chains achieve a greater extent of interpenetration into the 21k base network as compared to the 23k base network. The larger mesh size of the 21k network seems to favor this greater interpenetration.

Values of $3[f^*]_{\alpha=1}$ extrapolated from the Mooney–Rivlin plots are also listed in Table 2. These values should in theory match the elongational modulus E obtained from the initial slope of f versus α. In general, there is a reasonable consistency between the two values except for the IPNs from the 2.3k short chains. We suspect that the discrepancies are due to errors in the extrapolation of the Mooney–Rivlin plots.

4. Conclusion

We have prepared six series of IPNs with three different short chains (molar mass 800, 2300, 5700 g mol^{-1}) interpenetrated with one of the two long-chain base networks (molar

Table 2
Mooney–Rivlin constants

M_n of base network	Vol% of trimethoxy-terminated PDMS (initial solvent) in base network	M_n of short chain	mol%, mass% of short chain	E (MPa)	$2C_2$ (MPa)	$2C_1$ (MPa)	$3[f^*]_{\alpha=1}$ (MPa)
23k	0	800	0	0.63	0.11	0.12	0.69
			70, 6.1	0.66	0.11	0.14	0.74
			80, 13	0.68	0.12	0.16	0.83
			90, 23	0.87	0.10	0.20	0.90
			92.5, 30	0.94	0.12	0.22	1.01
			95, 40	1.04	0.15	0.34	1.47
			100	3.69	0.32	0.98	3.90
		2.3k	0	0.46	0.11	0.10	0.63
			70, 19	0.61	0.14	0.17	0.93
			80, 28	0.71	0.13	0.26	1.17
			90, 47	0.94	0.11	0.22	0.99
			92.5, 55	1.03	0.11	0.24	1.06
			100	2.19	0.29	0.43	2.16
		5.7k	0	0.63	0.12	0.12	0.70
			50, 21	0.80	0.12	0.17	0.88
			60, 29	0.84	0.14	0.18	0.96
			67, 33	0.88	0.11	0.18	0.87
			73, 38	0.95	0.11	0.22	0.97
			100	1.88	0.202	0.42	1.88
21k	50	800	0	0.22	0.04	0.04	0.25
			92.5, 32	0.52	0.05	0.17	0.66
			95, 45	0.71	0.07	0.18	0.74
			97.5, 62	0.96	0.08	0.23	0.94
			98.5, 74	1.11	0.08	0.33	1.23
			99, 81	1.36	0.04	0.42	1.4
			100	3.69	0.32	0.98	3.9
		2.3k	0	0.22	0.04	0.04	0.25
			80, 26	0.47	0.05	0.11	0.50
			85, 37	0.53	0.07	0.20	0.81
			90, 49	0.66	0.08	0.20	0.83
			95, 67	0.71	0.09	0.18	0.82
			100	2.19	0.29	0.43	2.16
		5.7k	0	0.22	0.04	0.04	0.25
			60, 29	0.25	0.03	0.05	0.26
			65, 30	0.40	0.04	0.07	0.35
			70, 36	0.50	0.07	0.11	0.54
			75, 44	0.65	0.09	0.15	0.72
			80, 52	0.71	0.10	0.20	0.89
			100	1.88	0.20	0.42	1.88

mass 23,000 or 21,000 g mol^{-1} in 50% solvent). The modulus–swelling relationship of the IPNs followed a scaling law identical to that for unimodal PDMS elastomers previously reported. This result supports the hypothesis that load can be transferred effectively between the networks. Therefore, the networks in an IPN cannot be considered as energetically independent, as assumed by Okumura [4]. Our attempt to correlate the relationship between toughness enhancement and property/composition factors of the IPNs using the equal-stress or equal-strain model for IPN of Okumura has not been successful. Our results show that the toughness improvement is achieved at moderate mol% of short chains. An empirical model based on fracture mechanics seems to provide a reasonable way to correlate the experimental results and shows a complex relation between toughness enhancement in IPN with composition, modulus and maximum stress of the individual components of the interpenetrated network.

Acknowledgements

This work was supported in part by NSF Polymers Program under grant DMR-0349952. This work made use of the Cornell Center for Materials Research supported through the National Science Foundation Materials Research Science and Engineering Centers program (Award DMR-0079992). We acknowledge useful discussion with T.M. Duncan, F. Escobedo, A. Batra and G. Genesky.

References

[1] Sperling LH, Mishra V. Polym Adv Technol 1995;7:197.
[2] Clarson SJ, Fitzgerald JJ, Owen MJ, Smith SD. Silicones and silicone-modified materials. In: ACS symposium series, vol. 729, Washington DC; 2000.
[3] Mark JE, Ning YP. Polym Eng Sci 1985;25(14):824.

[4] Okumura K. Europhys Lett 2004;67(3):470.
[5] Lee C, Frye C, Johannson O. Polym Prepr 1969;10:1361.
[6] Lee C. US patent 3,445,426; 1969.
[7] Lee C, Johannson O. J Polym Sci Polym Chem 1976;14:729.
[8] Lee C, Mark O, Johannson O. J Polym Sci Polym Chem 1976;14:743.
[9] Lapp A, Herz J, Strazielle C. Makromol Chem 1985;186:1919.
[10] Lorente M, Mark J. Macromolecules 1980;13:681.
[11] Valles E, Macosko C. Macromolecules 1979;12:521.
[12] Meyers K, Bye M, Merrill E. Macromolecules 1980;13:1045.
[13] Patel SK, Malone S, Cohen C, Gillmor JR, Colby RH. Macromolecules 1992;25:5241.
[14] Sivasailam K, Cohen C. J Rheol 2000;44(4):897.
[15] Weiss P, Herz J, Rempp P. Makromol Chem 1970;135:249.
[16] Christensen RM. Mechanics of composite materials. NY: John Wiley & Sons; 1979. p. 107–8.
[17] Paul B. Trans AIME 1960;218:36.
[18] Rubinstein M, Colby RH. Polymer physics. New York: Oxford University Press; 2003.
[19] Mark JE. Adv Polym Sci 1982;44:1.
[20] Anderson TL. Fracture mechanics—fundamentals and applications. Boca Raton: CRC Press; 1991.
[21] Gong JP, Katsuyama Y, Kurokawa T, Osada Y. Adv Mater 2003;15:1155.
[22] Na YH, Kurokawa T, Katsuyama Y, Tsukeshiba H, Gong JP, Osada Y, et al. Macromolecules 2004;37:5370.